

Do TMS evoked responses measured from scalp and hand represent the same cortical mechanisms?

Mana Biabani ^a, Alex Fornito ^a, James P. Coxon ^b, Ben D. Fulcher ^{a, c}, Nigel C. Rogasch ^{a, d, e}

^a Brain, Mind and Society Research Hub, School of Psychological Sciences, Monash Biomedical Imaging, Turner Institute for Brain and Mental Health, Monash University, VIC, Australia

^b School of Psychological Sciences, Turner Institute for Brain and Mental Health, Monash University, Clayton, VIC, Australia

^c School of Physics, The University of Sydney, Sydney, NSW, 2006, Australia

^d Discipline of Psychiatry, Adelaide Medical School, University of Adelaide, Adelaide, SA, Australia

^e South Australian Health and Medical Research Institute (SAHMRI), Adelaide, SA, Australia

Abstract

Introduction: Transcranial magnetic stimulation (TMS) is a powerful tool to investigate local cortical circuits and broader neural networks. Paired-pulse TMS (ppTMS) paradigms are commonly employed to study excitatory/inhibitory neurotransmissions in motor circuits across time by assessing changes in motor-evoked potentials (MEPs) using electromyography (EMG). The combination of TMS with electroencephalography (EEG) has the capacity to extend this work outside the motor system by focusing on TMS-evoked potentials (TEPs) across both space and time as the measurable output of brain stimulation. However, the relationship between these two putative outputs of TMS effects - MEPs and TEPs - remains unclear. **Aim:** To investigate whether the same neural populations are responsible for fluctuations in MEPs with ppTMS as the TEP waveform following single pulse TMS (spTMS). **Methods:** Twenty-four healthy participants received intra-hemispheric and interhemispheric (dual-coil) ppTMS, with different inter-pulse intervals, conditioning intensities, and TMS pulse waveforms over the motor cortex, while EMG was recorded from first dorsal interosseous muscles. EEG was also recorded in response to spTMS with the same intensity and location as the conditioning pulses in ppTMS-EMG. Additionally, TMS was applied to the shoulder as a multisensory control condition. The relationship between ppTMS-EMG and spTMS-EEG were evaluated using metrics sensitive to both the shape and amplitude of the signals. **Results:** The fluctuations in cortical excitability following suprathreshold TMS were correlated in shape, but not amplitude, when measured with ppTMS-EMG and TMS-EEG. This relationship was observable only after reversing the

polarity of short latency TEPs (~ 60 ms). For interhemispheric measures, suppressing sensory potentials in TEPs was required to discern the relationship between the two signals.

Conclusion: The relationship between MEP and TEP measures suggests both signals reflect activity from overlapping neural populations. This finding establishes a fundamental link between TEP peaks and periods of net excitation/inhibition observed with ppTMS-EMG in both the stimulated motor cortex and connected cortical regions.

Introduction

Transcranial magnetic stimulation (TMS) is a non-invasive brain stimulation method capable of activating cortical neurons across the intact scalp in humans [1]. A single TMS pulse depolarises a combination of excitatory and inhibitory neurons in the underlying cortical tissue, resulting in fluctuating periods of net excitation and inhibition that can last for several hundred milliseconds following stimulation [1]. In addition to local cortical circuits, TMS also indirectly activates cortical regions that are structurally connected to the stimulated region, resulting in a complex cascade of neural firing through large-scale cortical networks [2]. As such, TMS has emerged as a powerful tool to study excitatory and inhibitory neurotransmission in local and connected brain regions in humans.

The local and remote effects of TMS are typically quantified using some observable output. In the most common method, TMS of primary motor cortex (M1) is coupled with electromyographic (EMG) recordings of a peripheral muscle targeted by the stimulated region. A single TMS pulse to M1 can result in a measurable muscle response known as a motor-evoked potential (MEP), the amplitude of which provides a measure of corticomotoneuronal excitability at the time of stimulation. Paired-pulse TMS (ppTMS) EMG paradigms are used to probe TMS-evoked changes in net excitation of motor-related cortical circuits across time, although the excitability of spinal circuits may also contribute [1, 3, 4]. In these paradigms, a conditioning stimulus is delivered over M1 followed by a test stimulus (TS) after a given interval. The amplitude of the resulting conditioned MEP is then compared against the MEP induced by a TS alone to assess the excitatory or inhibitory effects of the conditioning stimulus [1, 5, 6]. In addition to local assessments of the stimulated M1, ppTMS-EMG can probe the interactions of M1 with other cortical regions by employing a second coil and applying the conditioning stimulus to an interconnected brain region (e.g., contralateral M1)[7]. Although ppTMS-EMG provides a wealth of information about local and inter-regional cortical circuits,

this technique is limited to the assessments of motor cortex and provides an indirect measure of cortical activity.

The second and more recently emerging method combines TMS with electroencephalography (EEG), which measures fluctuations in cortical excitability across the scalp. The brain's response to single-pulse TMS (spTMS) appears as a sequence of reproducible voltage deflections in TMS-evoked EEG potentials (TEPs) over a period of 0 to 500 ms post-stimulus, at the site of stimulation and in interconnected brain regions [2, 8, 9]. M1 TEPs have been commonly characterised by seven peaks: N15, P30, N45, P60, N100, P180, and N280 [10, 11]. In general, EEG deflections such as TEPs are thought to reflect synchronous changes in postsynaptic potentials across large populations of neurons. Therefore, similar to ppTMS-MEPs, changes in their amplitude can be used to quantify fluctuations in intracortical excitability following a TMS pulse. However, in contrast to MEPs, the polarity of TEPs does not provide a clear indication of the net excitation/inhibition of cortical circuits. This is because excitatory/inhibitory inputs to either the apical or basal dendrites of layer 5 neurons, which are thought to contribute most to the EEG signal, can have opposite effects on EEG polarity (see Ref. [12] for a comprehensive explanation of polarity in EEG). To make inferences about neurophysiological correlates of TEPs, other markers of cortical excitation/inhibition are commonly used as benchmarks, against which TEP components are evaluated. A growing body of evidence from pharmacological and behavioural TMS-EEG studies has linked certain peaks of M1 TEPs to periods of net excitation (e.g. N15, P30) and inhibition (e.g. N45, N100) [13-17]; however, the evidence is far from conclusive [18]. Furthermore, recent evidence suggests that some of the TEP signal may result from indirect sensory input, evoked by the TMS pulse, further complicating interpretation of TEP peaks [19, 20].

Taken together, both ppTMS-EMG and spTMS-EEG measure periods of net excitation and inhibition across time in response to a TMS pulse. However, it remains unclear whether the same population of cortical neurons is responsible for fluctuations in excitability measured by MEPs and TEPs. Preliminary evidence suggests a relationship between the amplitude of MEPs and the shape of TEPs by showing a correlation between MEP inhibition following ppTMS at an ISI of 100 ms and the slope of the N100 TEP (70-95 ms) [14]. However, whether this finding holds for other ISIs, and for TEP amplitude, has not been investigated. The aim of this study was to explore the relationship between EEG and EMG measures of intracortical responses to TMS across time, using metrics sensitive to both the shape and amplitude of the signals. We

conducted two experiments and examined both local and interhemispheric responses to TMS over M1 at different intensities: sub- and supra-threshold. We also assessed the generalizability of the results by examining different stimulation waveforms (biphasic and monophasic) and evaluated the specificity of the findings to cortical stimulation by testing them against a sensory control condition.

Methods

Participants

Two experiments were conducted for this study. In Experiment I, 20 (24.50 ± 5 years; 14 females) right-handed healthy individuals were examined and in Experiment II, 16 (25 ± 6 years; 11 females) individuals were examined. Twelve subjects participated in both experiments. All subjects were screened for any contraindications to TMS [21], and provided written consent to the experimental procedure, which was approved by the Monash University Human Ethics Committee in accordance with the declaration of Helsinki. The TMS-EEG data from this study was also used in our recent publication investigating sensory contributions to TEPs [19]. Participants were seated comfortably in an adjustable chair, with their elbows resting on the armrests and forearms pronated and supported on a pillow on their laps. They were instructed to keep their eyes open, look at a black screen in front of them and stay relaxed.

TMS

In Experiment I, biphasic TMS (anterior-posterior/posterior-anterior) pulses were administered to the left M1 using a figure-of-eight coil (C-B60) connected to a MagPro X100+Option stimulator (MagVenture, Denmark). Stimulations were applied over the optimal point for the stimulation of first dorsal interosseous (FDI), where the suprathreshold pulses consistently produced largest MEPs [22]. This location was digitally marked on each individual's T1 scan using a neuronavigation system (BrainsightTM 2, Rogue Research Inc., Canada) to ensure the consistency of coil positioning across stimulation blocks. Resting motor threshold (rMT) was determined as the minimum stimulation intensity required to evoke MEPs stronger than $50 \mu\text{V}$ in at least 5 of 10 successive trials [23]. Then, the intensity was gradually

increased until MEPs of ~1 mV were elicited in at least 10 consecutive trials (S1mV). All assessments and stimulations blocks were carried out with EEG cap on and the intensities are expressed as a percentage of maximum stimulator output (% MSO). Paired-pulse stimulations were delivered using both sub- and suprathreshold conditioning stimuli (80% and 120% rMT) and suprathreshold test stimulus (S1mV), and seven inter-stimulus intervals (ISIs): 15, 30, 45, 55, 100, 120, 180, and 220 ms. For MEPs, each subject received eight blocks of 40 stimuli over left M1 including one block of 40 pulses at S1mV as unconditioned stimulations, and seven blocks of 40 ppTMS (20 pulses for each conditioning intensity at each ISI) as conditioned stimulations. The stimulation intensities within each block were controlled by the MATLAB-based MAGIC (MAGnetic stimulator Interface Controller) Toolbox [24]. To examine TEPs, participants received four blocks of 50 spTMS with two intensities of 80% and 120% rMT (100 pulses in total for each intensity), while EEG was continuously recorded.

In Experiment II, we applied both uni- and bi-hemispheric stimulations. TMS was performed using a Magstim 200² stimulator (Magstim Company, UK) producing single monophasic pulses in posterior-anterior direction. For ppTMS a second Magstim 200² stimulator equipped with a BiStim² timing module (Magstim Company, UK) was added. The stimulators were triggered by Signal software (V6) and CED data acquisition interface (Cambridge Electronic Design, Cambridge, UK). Uni-hemispheric stimulations were delivered to the left M1 through a figure-of-eight D70² Coil (Magstim Company Ltd., Whitland, UK), and for bi-hemispheric stimulations a smaller second coil (D50 Alpha; Magstim Company Ltd., Whitland, UK) was positioned over the right M1. Using a smaller coil allowed positioning of both coils over the head. All of the baseline measurements and intensity settings were performed for each coil separately. Paired-pulse stimulations were delivered using suprathreshold conditioning stimulus (120% rMT) and TS (S1mV) with eight ISIs: 10, 20, 30, 40, 50, 100, 150, and 200 ms. For uni-hemispheric tests, TMS was applied over the left M1 and MEPs were recorded from right FDI. For bi-hemispheric TMS, conditioning stimulus was also applied to the left M1. However, both conditioned and unconditioned TS (S1mV) were administered to right M1 while MEPs were recorded from left FDI. For MEPs, each individual received five blocks of uni-hemispheric and five blocks of bi-hemispheric TMS. Each block consisted 40 ppTMS (5 for each ISI) and 10 spTMS (S1mV), pseudo-randomly distributed. For TEPs, participants received 75 single pulses over left M1 at 120% rMT while EEG was continuously acquired.

For both experiments, white noise was played to the participants through inserted earphones and a thin layer of foam was attached underneath the coil during all of the stimulation blocks [25] to attenuate the effect of peripherally-evoked potentials (PEPs) (e.g. auditory evoked potentials from the click and somatosensory evoked potentials from coil vibration) on TEPs. Additionally, as a control condition, each participant received 100 suprathreshold TMS pulses over the left shoulder to elicit PEPs due to TMS coil clicks and tapping sensation, without transcranially stimulating the brain [19]. While this control is likely suboptimal for somatosensory activation (e.g. shoulder vs scalp), we have previously demonstrated that the resulting sensory signal accounts for much of the fronto-central N100/P180 complex observed in motor TEPs [19, 26]. For each participant, the block order was pseudo-randomized and regular breaks were given between blocks. Within each block, the different types of pulses were also given pseudo-randomly with the intervals jittered between 4 and 6 s.

EMG

EMG was recorded from the left and right FDI using bipolar Ag-AgCl surface electrodes (~2 cm apart) positioned in a belly-tendon montage. A ground electrode was fixed on the dorsum of the hand over the midpoint of the third metacarpal bone for each side. EMG was band-passed filtered at 10 to 1000 Hz, amplified 1000 times, sampled at 5 kHz, epoched around the stimulation pulse (−200 to 500 ms), and recorded on a computer for offline analyses. EMG data were processed offline using Labchart 8 (ADIstruments, Sydney, Australia). First, the trials with pre-stimulus muscle contractions (up to 100 ms) were identified and excluded following visual inspections. Then, the average of peak-to-peak values of MEPs evoked by each type of stimulation were calculated for each subject. Finally, the strength of inhibition or excitation was calculated as the percentage of the mean MEPs evoked by conditioned pulses (ppTMS) over the mean MEPs evoked by unconditioned pulses (spTMS, S1mV).

EEG

EEG was continuously acquired through a TMS-compatible EEG system (SynAmps², Neuroscan, Compumedics, Australia) using 62 Ag/AgCl ring electrodes, arranged in an elastic

cap according to the standard 10–20 layout (EASYCAP, Germany). The positions of the electrode were digitized and co-registered to each individual's T1 weighted MR scan in the neuronavigation system. All the electrodes were grounded to AFz and online-referenced to FCz. EEG signals were amplified (1000 \times), low-pass filtered at DC–2000 Hz and digitized with a sampling rate of 10 kHz. The skin-electrode impedance level was kept below 5 k Ω throughout the recordings [11]. The signals were displayed and stored on a computer using the Curry8 software (Neuroscan, Compumedics, Australia). EEG data were preprocessed based on the method described in [27, 28], performed by custom scripts written in MATLAB (R2016b, The Mathworks, USA) using the functions provided by EEGLAB [29] and TESA [28] toolboxes. These scripts are available at: <https://github.com/BMHLab/TEPs-PEPs> and the pipeline has been described in detail in our recent publication [19]. For further analysis, we reduced the dimensionality of EEG by extracting the data from left and right M1. We chose C3 and C4 channels which have been identified as the scalp markers of the two motor cortices in 10-20 system [30, 31], and grouped them with their eight neighbouring electrodes. As such, the average of TEPs recorded at C3, FC1, CP1, FC5, CP5, C1, FC3, CP3, and C5 was calculated to represent the activity of left M1, and the average of the recordings at C4, FC2, CP2, FC6, CP6, C2, FC4, CP4, and C6 was taken as the activity of right M1. We also adopted a data driven approach (correlation-based hierarchical clustering) to define our region of interest. In this method, we used average linkage clustering on Spearman correlation between the temporal responses recorded by each pair of electrodes to cluster the channels into groups [32]. Spearman's correlation coefficients were used as the distance metric, and the clustering cut-off was set at a percentage of the maximum distance giving the highest Silhouette coefficient (an index for the quality of clustering ranging from -1 to 1 [33]).

Our pre-processed EMG and EEG data is freely available on figshare at <https://doi.org/10.26180/5cff2a0fc38e9> and raw data is also available upon request.

Statistical analysis

All statistical analyses were performed in MATLAB; all code is available at <https://github.com/BMHLab/TEPs-MEPs>. To examine the effect of different conditioning stimuli (80% and 120% rMT) on the size of MEPs induced by TS, we applied nonparametric Wilcoxon signed rank tests (as TEPs and MEPs were not normally distributed at all timepoints)

comparing the size of conditioned MEPs (induced by ppTMS) with unconditioned MEPs (induced by TS alone) at each ISI. To assess the relationship between EEG and EMG measures of cortical responses to TMS, we compared ppTMS-MEPs at each intensity of conditioning stimulus with the TEPs evoked by the same conditioning stimulus alone, adopting two main approaches. First, we examined Spearman's correlations between TEPs and MEPs at each point of time (each ISI) to see whether the amplitude of TEPs reflects the excitation or inhibition observed in MEPs. Second, we compared the shape of the two signals (patterns of signal fluctuations independent of overall amplitude) using two metrics: slope, and a shape-similarity metric (SSM). Slope was calculated as the mean first derivative of TEPs during the 30 ms preceding each timepoint, corresponding to the ISIs in ppTMS [14]. Spearman's correlations were then used to evaluate the relationship between the amplitude of ppTMS-MEPs and the slope of spTMS-TEPs, at each ISI. Slope analysis was not performed for ISIs shorter than 30 ms, due to insufficient EEG data (TEPs are contaminated by TMS-Pulse artefacts to 15 ms and were replaced by interpolated data during the pre-processing stage). For the same reason, we used a shorter time window for slope calculation for the ISI of 30 ms (15–30 ms). The SSM between MEPs and TEPs was calculated as the sum of the absolute differences between the MEPs and TEPs over all ISI time points, allowing an arbitrary proportional rescaling on TEP measurements:

$$SSM = \min_{\lambda > 0} \sum_{i=1}^t |M_i - \lambda T_i| \quad (1)$$

for a rescaling parameter, λ , across t time points, where M is MEP measurement, and T is TEP measurement. The formulation of SSM in terms of a rescaling allows it to be independent of the scales of measurement, and instead capture the similarity in relative variation (shape): lower SSM values indicate that M and T have similar shapes.

To examine whether a computed SSM value is significantly lower than what would be expected by chance, we randomly shuffled TEP and MEP data to compute a 1000-sample null distribution of SSM values. This null distribution was used to compute p -values for SSM directly. For group-level analysis, we calculated the sum of SSM values across all individuals and again evaluated the statistical significance as a permutation test, using the null distribution formed by sum of the SSM values from the individually permuted TEPs and MEPs. As TEP data before 15 ms is highly contaminated by artifacts, we excluded the latency of 10 ms for this

analysis. All statistical results were corrected for multiple testings across ISIs using the Benjamini-Hochberg false discovery rate (FDR) correction [34].

Results

The study protocol was well-tolerated by all participants and no adverse effects were reported. In Experiment I (MagVenture, Biphasic), rMT was 57 ± 9 %MSO and the amplitude for S1mV was 70 ± 12 %MSO. In Experiment II (Magstim Bistim, Monophasic), rMT and S1mV were 48 ± 7 and 60 ± 8 %MSO for left M1, and 58 ± 5 and 72 ± 8 %MSO for right M1, respectively.

EMG responses to ppTMS with different conditioning stimuli and ISIs

Fig. 1 illustrates the effects of sub- and suprathreshold conditioning stimuli on the amplitude of the MEPs evoked by TS (S1mV) with different intervals between pulses. For left M1 stimulation, the conditioning stimulus at 120% rMT showed very similar pattern of facilitation and inhibition between the two TMS pulse waveforms (mono- and biphasic). Both biphasic and monophasic ppTMS exhibited an early phase of facilitation (10–15 ms to 30 ms) followed by a long phase of inhibition (50–60 ms to 180–200 ms) (Fig 1A and B). The conditioning stimulus at 80% rMT produced a small facilitation observed at 15 ms. However, in the subthreshold condition, the magnitude of MEPs to conditioned TS did not statistically differ from the MEPs to TS alone, at any of the ISIs ($p > 0.05$). For inter-hemispheric stimulation, conditioning stimulus over left M1 reduced the MEPs evoked by the following TS over right M1 at ISIs of 10 to 50 ms, corresponding to the two phases of IHI [7].

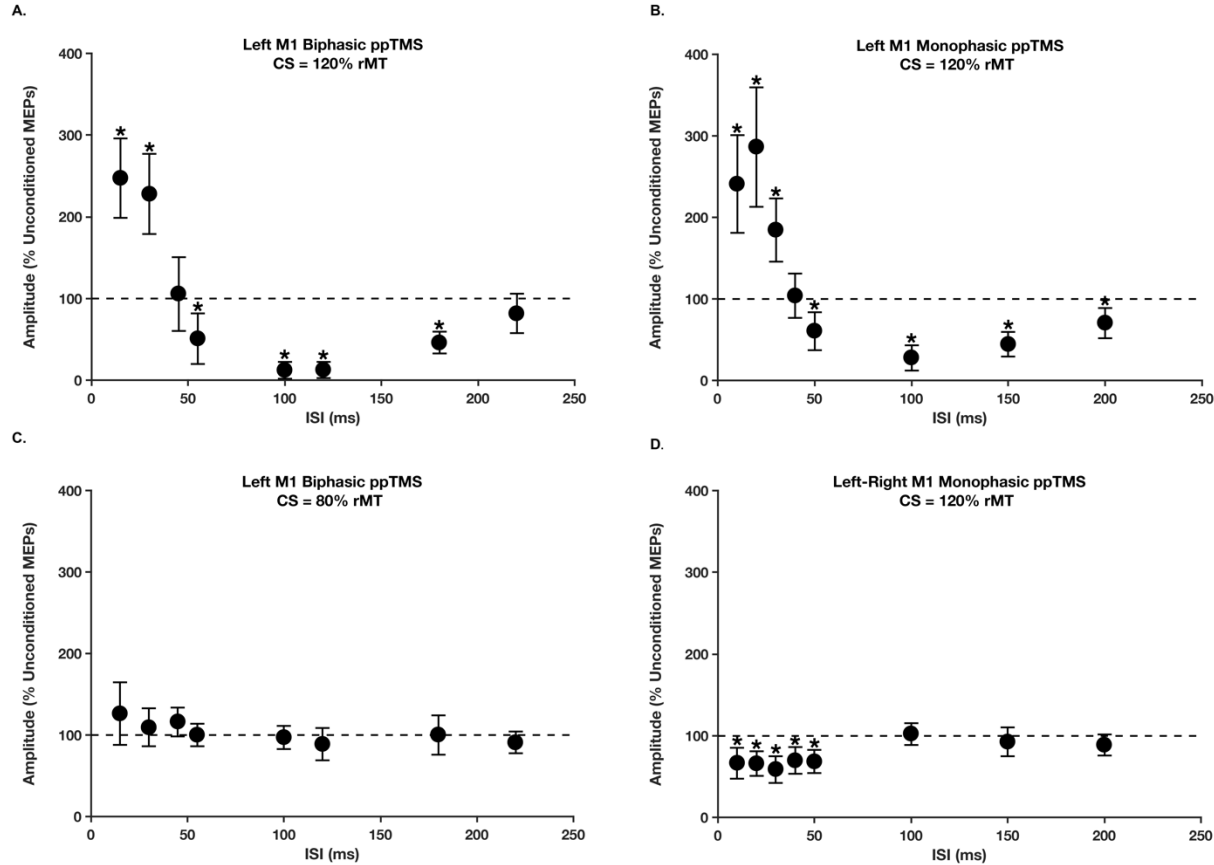


Figure 1: Changes in intracortical excitability in response to paired TMS pulses over M1 using different stimulation parameters. A-C) Both conditioning stimulus (CS) and test stimulus (TS) were administered to left M1 and MEPs were recorded from right FDI. D) CS and TS were applied over left and right M1, respectively, and EMG was recorded from left FDI. The solid circles represent the mean amplitude of conditioned MEPs expressed as a percentage of the mean MEP amplitude (across individuals) from TS alone. The error bars indicate 95% of confidence intervals assuming a Gaussian distribution. * indicate $p < 0.05$ comparing conditioned and unconditioned MEPs.

EEG responses to spTMS

Following suprathreshold stimulation over left M1, the local TEPs at the site of stimulation showed a sequence of strong deflections ($\sim \pm 5 \mu\text{V}$) with an early negativity around 20 ms followed by a period of positivity (from 30 to 80 ms) and a long period of negativity (from 80 to 220 ms), in both biphasic and monophasic conditions (Fig. 2). Subthreshold stimulation induced small deflections ($\sim \pm 1 \mu\text{V}$) strongest before 100 ms (Fig. 2A). The TEP for right M1 electrodes following left M1 stimulation showed an early positive peak around 30 ms ($\sim +3 \mu\text{V}$), followed by a period of negativity from 40 to 130 ms ($\sim -3 \mu\text{V}$) and then a large positive peak around 180 ms ($\sim +6 \mu\text{V}$) (Fig. 2B).

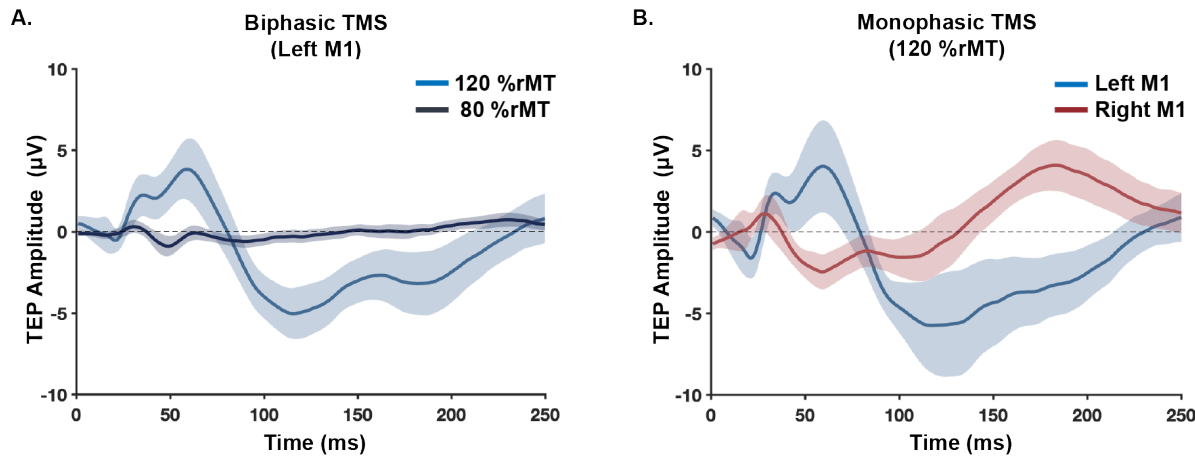


Figure 2: EEG recordings in response to biphasic (A) and monophasic (B) spTMS at two different intensities (80 and 120 %rMT) over left M1. For left M1 recordings, TEPs show the average of recordings at C3, FC1, CP1, FC5, CP5, C1, FC3, CP3, C5. For right M1 recordings, TEPs represent the average of recordings at C4, FC2, CP2, FC6, CP6, C2, FC4, CP4, C6.

Comparisons of TMS-induced intracortical responses recorded by MEPs and TEPs

Correlations of amplitudes

To test whether the amplitude of ppTMS-MEPs corresponds with the amplitude of spTMS-TEPs, we computed the Spearman correlation between the MEP amplitude and the TEP amplitude across participants at each time point. Correlation coefficients were not significant (corrected p value (p_{corr}) > 0.05 ; corrected across eight timepoints) at any of the time points evaluated (except for subthreshold TMS at ISI of 15 ms), suggesting that variability in the level of excitation shown by MEPs at each time point may not be predictive of changes in TEP amplitude (Table 1).

Table 1. Spearman correlations between ppTMS-MEPs and spTMS-TEPs at each point of time

| Biphasic condition | 15 ms | 30 ms | 45 ms | 55 ms | 100 ms | 120 ms | 180 ms | 220 ms |
|---------------------------------|---------------|--------------|--------------|--------------|--------------|---------------|---------------|---------------|
| Left M1 (suprathreshold) | 0.07 | -0.18 | 0.29 | 0.08 | 0.15 | 0.22 | 0.08 | 0.003 |
| Left M1 (subthreshold) | -0.63* | 0.28 | 0.53 | -0.20 | 0.46 | 0.33 | -0.34 | 0.45 |
| Monophasic condition | 10 ms | 20 ms | 30 ms | 40 ms | 50 ms | 100 ms | 150 ms | 200 ms |

| | | | | | | | | |
|--------------------------------------|---|--------|-------|-------|-------|------|-------|-------|
| Left M1 (suprathreshold) | - | 0.17 | -0.08 | -0.09 | 0.08 | 0.22 | 0.52 | 0.03 |
| Right M1 (suprathreshold) | - | -0.008 | -0.10 | -0.34 | -0.48 | 0.33 | -0.19 | -0.12 |

Time points represent the ISIs in ppTMS, the time points at which the correlations between TEPs and MEPs amplitudes were calculated. In monophasic conditions TEPs at 10 ms was excluded from this analysis due to the contamination of EEG responses to TMS pulse artefacts. *Indicates $p_{corr} < 0.05$ or significant correlation after FDR correction for multiple timepoints.

Comparisons of TEPs pattern and MEPs amplitude (slope analysis)

To test whether the pattern of TEPs mirrors the amplitude of paired pulse MEPs, we computed the Spearman correlation coefficient between MEP amplitude and the slope of change (mean derivative) in TEPs 30 ms preceding each time point. After FDR correction (for multiple timepoints), we did not find significant correlations at any of the time points and/or conditions evaluated, although responses to subthreshold stimulations showed relatively high relationships at all time points (Figs S1–3). Fig. 3 suggests that the weak correlations observed in the suprathreshold condition are at least driven by a methodological constraint. In TMS-EMG, conditioned MEPs are measured as a percentage of unconditioned MEPs and have a ceiling of inhibition at -100%; whereas, EEG measures are not confined to a specific range. Therefore, in the presence of strong inhibition (e.g., 100 ms), MEPs plateau at -100% and cannot follow the unconstrained changes observed in TEPs (Fig. 3).

Since choosing the window of 30 ms could cause interfering effects between the neighbouring peaks (30, 45, and 55 ms), we measured the slopes from shorter time windows of 10 ms, and again found no significant correlations (all $p_{corr} > 0.05$). To replicate the method used in a previous study [14], we pooled the measures from the two intensities of biphasic condition and found strong positive correlations at ISIs of 100 ms ($r = 0.75$, $p_{corr} = 1 \times 10^{-6}$) and 120 ms ($r = 0.49$, $p_{corr} = 0.005$). There was also some evidence for a negative correlation at 55 ms ($r = -0.35$, $p_{corr} = 0.06$), which is likely to be mainly driven by the responses to subthreshold TMS (Fig. 3). In line with previous reports, this analysis provides preliminary evidence that the shape of some parts of the TEP signal following spTMS correlates with changes in MEP amplitude following ppTMS. Interestingly, the relationship between ppTMS MEPs and TEPs appears to change direction between early signals (e.g., 55 ms) and later signals (e.g., 100–120 ms).

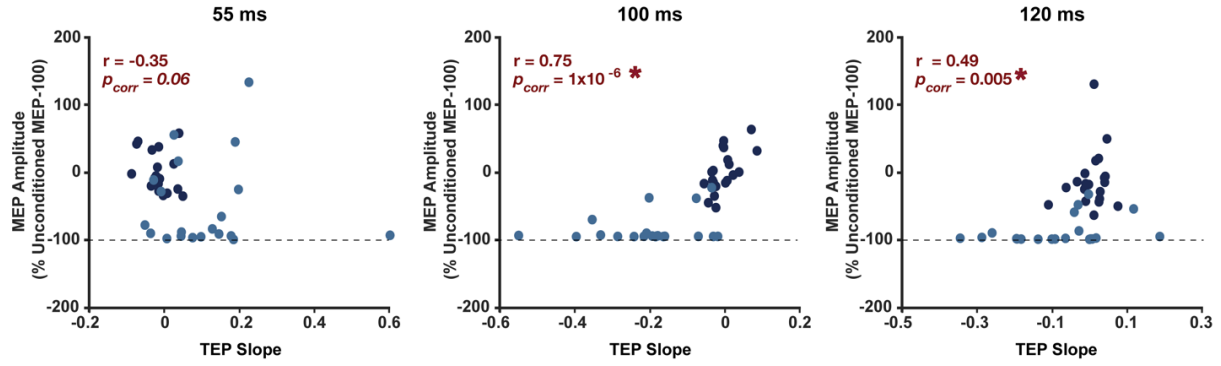


Figure 3: Spearman's correlation between MEPs amplitude and slope of TEPs at three different time points. TEPs and MEPs are responses to both subthreshold (dark blue circles) and suprathreshold (light blue circles) intensities of biphasic stimulation condition. The horizontal dash line shows the minimum level of inhibition measured in MEPs. * indicates $p_{corr} < 0.05$.

The relationship between TEPs and MEPs patterns (SSM measurement)

Instead of focusing on individual points in time, we next tested whether overall shape regardless of amplitude was similar between ppTMS-MEPs and spTMS-TEPs by calculating the SSM between the two signals. We found that, the two patterns were not more similar than would be expected by chance for any of the evaluated conditions (all $p > 0.05$).

Looking closely at the overlaid TEP and MEP patterns in the suprathreshold conditions (Fig. 4A and 4C), a notable divide is evident between the TEP-MEP relationships across time. Before ~ 60 ms, fluctuations in MEPs and TEPs followed the same pattern but with opposite polarity, whereas after ~ 100 ms the two responses showed the same pattern and direction. Given that (i) the polarity of the EEG is not necessarily indicative of either net excitation or inhibition [12], and (ii) the slope analysis suggested the relationship between ppTMS-MEPs and TEPs might switch over time (fig 3), we switched the polarity of EEG signals at the earlier phase for each individual and re-measured the relationship between TEPs and MEPs as described before. After the polarity reversal of the early TEP response, the SSM between the patterns of the two responses substantially improved for the suprathreshold biphasic condition ($p_{corr} = 0.008$; corrected for before/after polarity reversal), and the suprathreshold monophasic condition ($p_{corr} = 0.04$) (Figs 4). This result suggests that the relationship between the polarity of EEG and cortical excitation may alter over time, which, in turn, affects the shape of TEPs and conceals the relationship between the two signals.

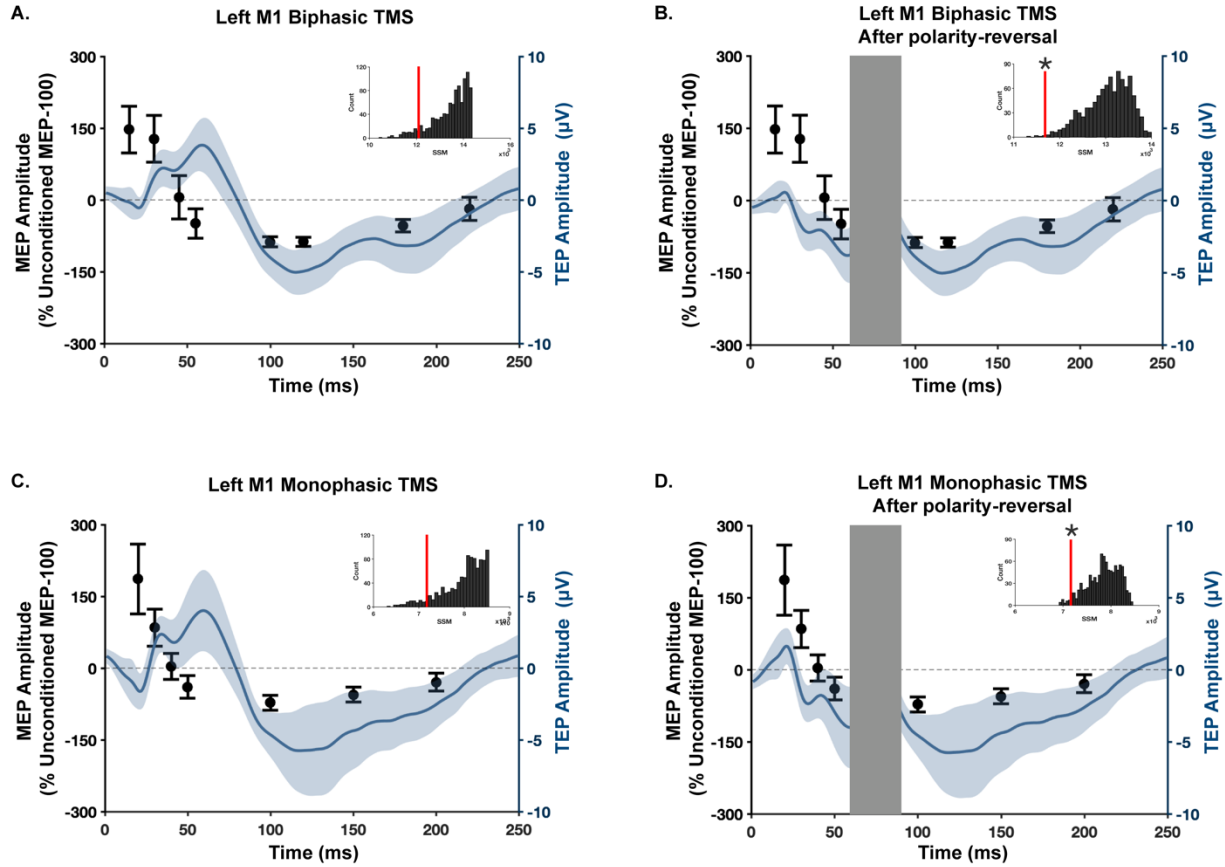


Figure 4: Comparisons of the intracortical fluctuations recorded by TEPs and MEPs in response to different stimulations waveforms over left M1 and the effect of polarity on the relationship between the two measures. A-B) Responses to suprathreshold biphasic TMS. C-D) Responses to suprathreshold monophasic TMS. The line graphs show the mean of EEG recordings at left M1 (the average of recordings at C3, FC1, CP1, FC5, CP5, C1, FC3, CP3, C5) and the shaded areas represent the 95% of confidence intervals, before (A, C) and after (B, D) reversing the polarity at 0 to 60 ms. The solid circles represent the mean amplitude of conditioned MEPs (recorded at right FDI) expressed as a percentage of the mean MEP amplitude from TS alone and the error bars indicate 95% of confidence intervals. The grey vertical bars show the window of time between 60 ms and 100 ms, when the effect of polarity could not be examined due to the lack of EMG data. The imbedded plots depict the distribution of group sum of SSMs from randomly shuffled TEPs and MEPs (the horizontal axis represents the measured SSM and the vertical axis shows the frequency of each SSM value). The red line shows the group sum of the result SSM. * indicates that $p_{corr} < 0.05$ (permutation test) suggesting a significant similarity between the two patterns.

Next, we tested whether the ppTMS-MEPs, which represent cortical responses to TMS over M1, were exclusively related to the EEG responses evoked by TMS, but not to other types of event-related potentials. To test the specificity of our findings to TMS activation, we assessed whether the shape of PEPs induced by shoulder stimulation were related to paired-pulse MEP shapes. We tested both monophasic and biphasic pulses and did not find any significant similarity between PEPs and MEPs before or after the polarity reversal (all $p_{uncorr} > 0.05$) (Fig. 5).

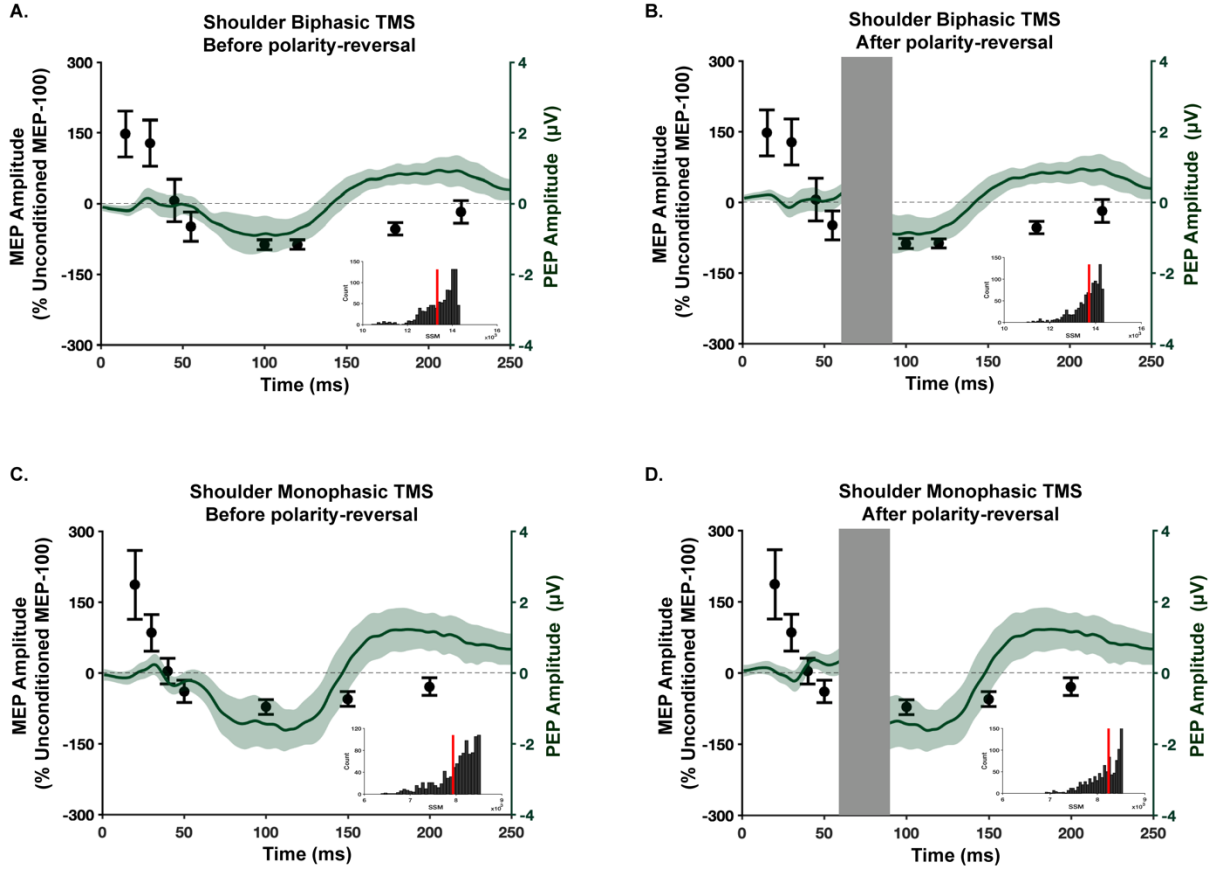


Figure 5: Effect of reversing the polarity of short latency EEG (<60 ms) on the relationship between PEPs (EEG responses to TMS over shoulder) and ppTMS-MEPs using different stimulations waveforms. A-B) Responses to suprathreshold biphasic TMS. C-D) Responses to suprathreshold monophasic TMS. The line graphs show the mean of EEG recordings at left M1 (the average of recordings at C3, FC1, CP1, FC5, CP5, C1, FC3, CP3, C5) and the shaded areas represent the 95% of confidence intervals, before (A, C) and after (B, D) reversing the polarity at 0 to 60 ms. The solid circles represent the mean amplitude of conditioned MEPs (recorded at right FDI) expressed as a percentage of the mean MEP amplitude from TS alone and the error bars indicate 95% of confidence intervals. The grey vertical bars show the window of time between 60 ms and 100 ms, when the effect of polarity could not be examined due to the lack of EMG data. The imbedded plots depict the distribution of group sum of SSMs from randomly shuffled TEPs and MEPs (the horizontal axis represents the measured SSM and the vertical axis shows the frequency of each SSM value). The red line shows the group sum of the result SSM. For all of the conditions, the resultant SSMs were found within the range of 95% of the permutation-generated SSMs, suggesting that the measured similarities between PEPs and MEPs are not different from that would be expected by chance, before and after polarity reversal.

Next, we tested whether the relationship between MEPs and TEPs was specific to the motor cortex by evaluating the distribution of SSM between the two response patterns across the scalp. We also grouped the channels from four other regions of interest (ROIs) including contralateral M1, frontal (FPz, FP1, FP2, AF3, AF4), central (Cz, FC1, FC2, CP1, CP2, C1, C2, CPz), and

occipital (PO2, O1, O2, P1, P2, Pz, PO3, PO4, Oz) sites and measured their similarity with pptMS-MEPs. After the polarity reversal the minimum SSM (maximum similarity) between TEPs and MEPs shifted more towards the stimulation site (Fig. 6), and none of the other regions of interest showed similarity with MEPs before or after switching polarity ($p_{uncorr} > 0.05$).

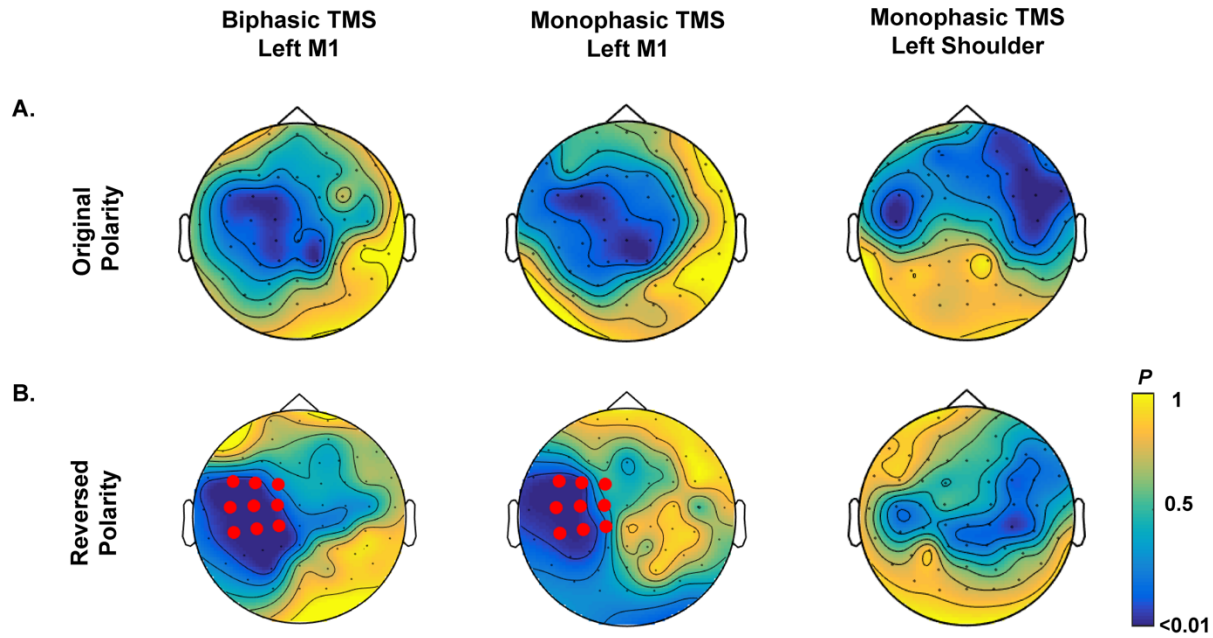


Figure 6: Site specificity of the relationships between EMG (right FDI) and EEG, before and after reversing the polarity of short latency EEG recordings (< 60 ms). A-B) Distribution of the p values from SSM calculations for EEG and EMG measures before (A) and after (B) the polarity reversal. Lower p values (darker colors) indicate more similarity. Among the five evaluated ROIs including left M1 (C3, FC1, CP1, FC5, CP5, C1, FC3, CP3, C5), right M1 (C4, FC2, CP2, FC6, CP6, C2, FC4, CP4, C6), frontal (FPz, FP1, FP2, AF3, AF4), central (Cz, FC1, FC2, CP1, CP2, C1, C2, CPz), and occipital (PO2, O1, O2, P1, P2, Pz, PO3, PO4, Oz) sites, only TEPs from left M1 showed similarities with MEPs after polarity reversal (biphasic $p_{uncorr} = 0.004$, monophasic $p_{uncorr} = 0.02$, and biphasic $p_{corr} = 0.02$, monophasic $p_{corr} = 0.1$; corrected for five ROIs). Note also that there were no significant similarities between MEPs and the PEPs from shoulder stimulation.

Given that our regions of interest were derived *a priori* without knowledge of the data [35], we also adopted correlation-based hierarchical clustering method as a data-driven approach to generate regions of interest. This approach produced four distinct clusters for TEPs and two clusters for PEPs (Fig. 7A-D). Then, for each individual, we took the average of TEPs within each cluster (at each point of time) to compare with MEPs. As depicted in Fig. 7, the only strong relationship between MEPs and TEPs was found after the polarity reversal (< 60 ms) and exclusively at the cluster around the site of stimulation ($p_{corr} = 0.01$; corrected for four clusters).

A similar result was obtained in the monophasic condition (Fig. S4). We also grouped the PEP data following shoulder stimulation based on the two clusters defined by PEPs and the four clusters specified by TEPs, none of which showed similarities with ppTMS-MEPs ($p_{uncorr} > 0.05$) (Fig. S5).

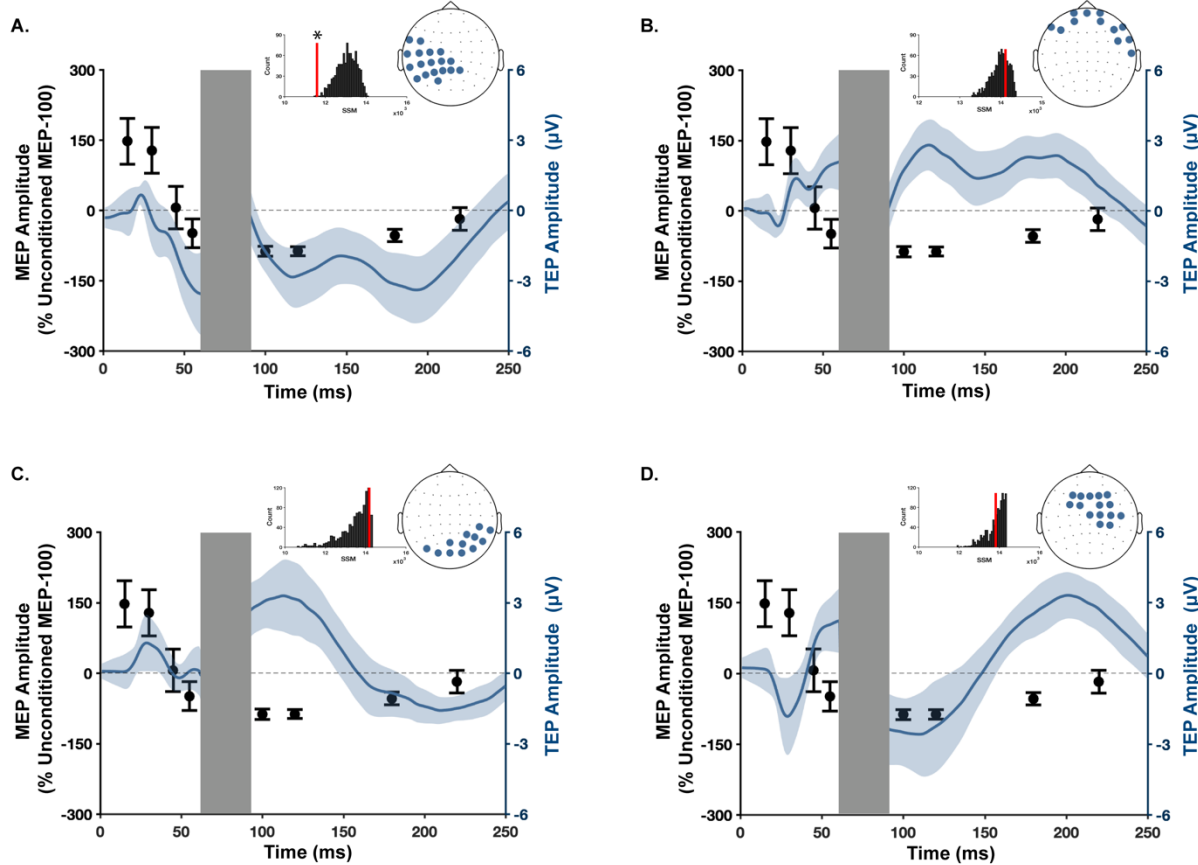


Figure 7: Site specificity of the relationships between EMG (right FDI) and EEG (ROIs defined by correlation-based hierarchical clustering method) after reversing the polarity of short latency EEG recordings (< 60 ms) in biphasic suprathreshold stimulations. Four clusters were identified in EEG recordings and the highlighted electrodes in scalp maps indicate the group of channels belong to each cluster. The line graphs show the mean of TEPs recorded at each cluster and the shaded areas represent the 95% of confidence intervals. The solid circles represent the mean amplitude of conditioned MEPs expressed as a percentage of the mean MEP amplitude from TS alone and the error bars indicate 95% of confidence intervals. The grey vertical bar shows the window of time between 60 ms and 100 ms, when the effect of polarity could not be examined due to the lack of EMG data. The bar plots depict the distribution of group sum of SSMs from randomly shuffled EEG and EMG responses (the horizontal axis represents the measured SSMs and the vertical axis shows the frequency of each SSM). The red line shows the group sum of the result SSMs. * indicates that $p_{corr} < 0.05$ (permutation test; corrected for four clusters) suggesting a significant similarity between the two patterns.

To further verify the robustness of the findings, we examined the time-specificity of the polarity changes. Since the window of 0–60 ms was chosen *post hoc*, we made the TEPs from M1 switch their polarity at different time windows searching for the maximum similarity with MEPs (minimum SSM). The window started from the first time point (corresponding to the first ISI), and added one ISI each time until the polarity of the whole signal was flipped. The results showed that the only window of time that resulted in a consistent similarity between the two measures for both monophasic and biphasic conditions was 0 to 60 ms (Fig. 8). This result was consistent between the two methods of ROI determination (Fig. 8). The window of 0–20 ms also showed low SSM especially in monophasic condition when M1 TEPs were selected from cluster analysis, but not from the *a priori* region of interest. Moreover, PEPs measured over M1 did not show any similarities with MEPs by flipping the polarity at any of the examined time-windows (Fig. 8).

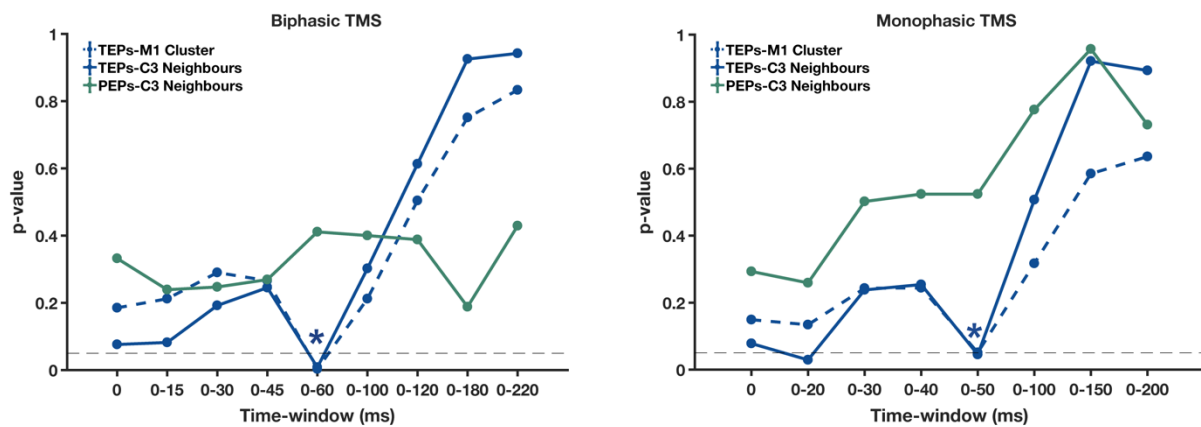


Figure 8: Testing the effect of polarity reversal at different time windows on the relationships between EMG (right FDI) and EEG (M1), for biphasic and monophasic conditions. No polarity change was applied at the time-window of 0. Blue lines represent p -values (permutation test) of the similarity between TEPs and MEPs and the green line depicts PEPs-MEPs similarities. The solid lines show that M1 responses were defined as the average of the potentials recorded by C3 and its eight neighboring electrodes (FC1, CP1, FC5, CP5, C1, FC3, CP3, C5). The dash line shows that TEPs were the average of the electrodes within the cluster around M1 defined by correlation-based clustering method. The horizontal dash line shows the level of significant similarity, $p_{uncorr} = 0.05$. * shows the time at which flipping the polarity of TEPs caused similarity between MEPs and TEPs (not PEPs) from both methods of ROI determination.

We also examined the effect of polarity on the relationship between the patterns of interhemispheric activity obtained from the two types of measurements but did not find a good match between the shape of the two responses (Fig. 9C). Also, changing the window of polarity-

reversal did not alter the results (Fig. S6). According to our previous findings [14], long latency EEG signals (>60 ms) recorded at the electrodes over the contralateral hemisphere can be highly contaminated by TMS-induced PEPs, despite adopting sensory attenuation measures (e.g., white noise and foam padding). Therefore, we examined whether suppressing PEPs in EEG recordings improves the SSM between the interhemispheric activity reflected in TEPs and MEPs. We used a spatial filter called signal-space projection with source-informed reconstruction (SSP-SIR), which shows a good trade-off between preserving the cortical responses directly evoked by TMS, while attenuating evoked cortical potentials resulting from the sensory experience of TMS [19]. Following attenuation of sensory potentials with SSP-SIR, a relationship between TEPs and MEPs was evident after reversing the polarity of the first 60 ms (Fig. 9D), similar to the local cortical responses. The hierarchical clustering method identified two main clusters in SSP-SIR cleaned data (clustering cut-off = 60%; silhouette scores of 0.8 ± 0.3) and only the cluster around right M1 showed significant SSM with MEPs ($p_{corr} = 0.04$; corrected for two clusters). The specificity of the relationship to M1 potentials was replicated when ROIs were determined based on neighbouring channels (Fig. 9), although the observed relationship was not as strong ($p_{uncorr} = 0.05$). We also examined the effect of PEP-suppression on the relationships between local responses to TMS (stimulations over left M1) and found a similar relationship as observed in unsuppressed data (Fig. S7). These findings suggest that suppressing PEPs with SSP-SIR preserves the shape of TMS-evoked neural activity at the site of stimulation, while revealing the propagation of TMS-evoked activity to contralateral areas previously obscured by PEPs.

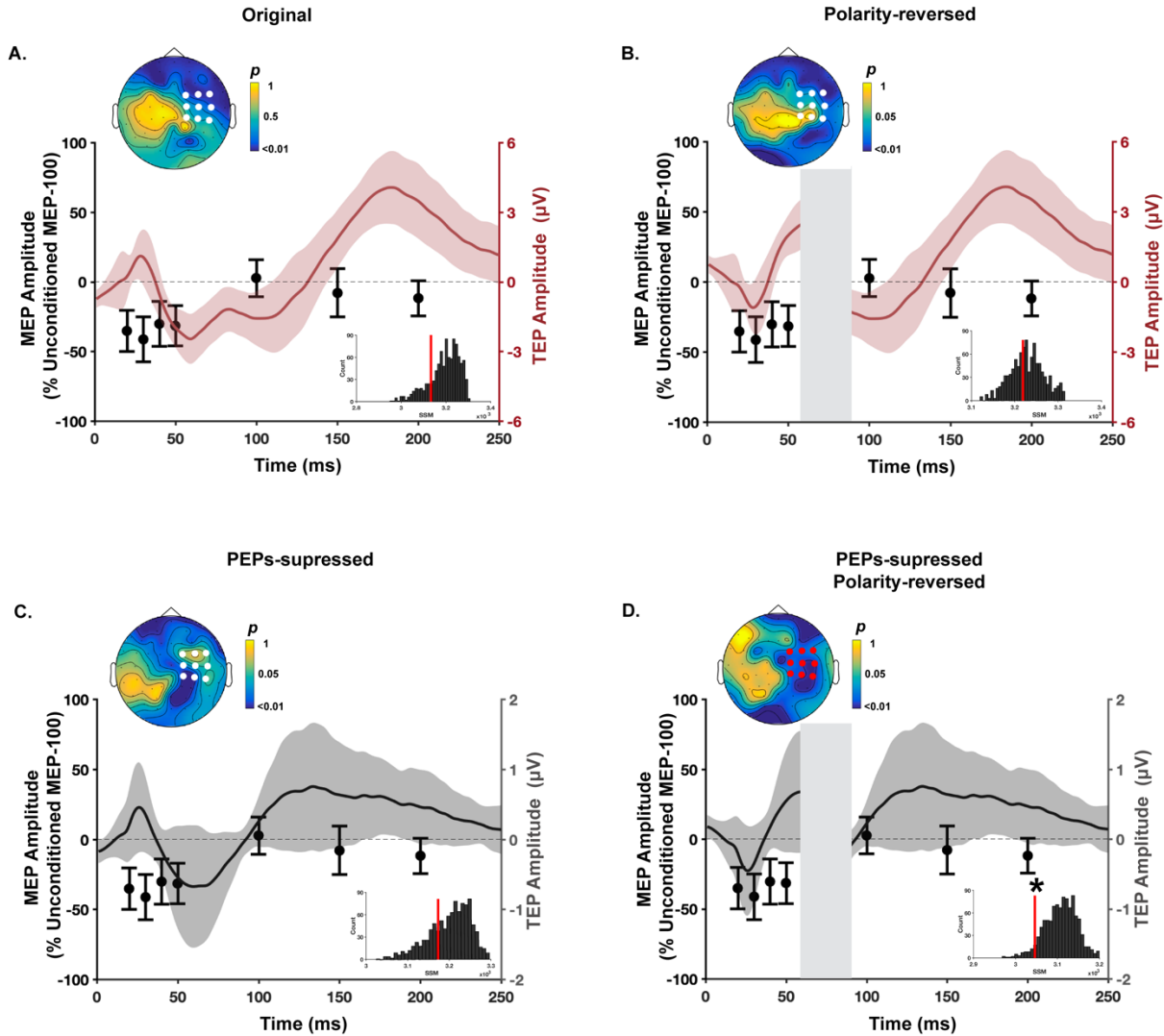


Figure 9: Relationships between interhemispheric responses to TMS (monophasic and suprathreshold) measured by EMG and EEG, before and after polarity-reversal and PEPs-suppression. A and B) Relationships between MEPs and TEPs before (A) and after (B) reversing the polarity of TEPs from 0 to 60 ms. C and D) Relationships between MEPs and PEPs-suppressed TEPs (using SSP-SIR) before (C) and after (D) polarity reversal. MEPs were recorded from left FDI following ppTMS with conditioning stimulus over left M1 and test stimulus over right M1. The solid black circles represent the mean amplitude of conditioned MEPs expressed as a percentage of the mean MEP amplitude from unconditioned conditioning stimulus and the error bars indicate 95% of confidence intervals. TEPs were the average of EEG responses to spTMS over right M1 recorded at the highlighted electrodes (C4, FC2, CP2, FC6, CP6, C2, FC4, CP4, C6). The line graphs show the average of TEPs recorded at the highlighted electrodes and the shaded areas represent the 95% of confidence intervals. The grey vertical bars show the window of time between 60 ms and 100 ms, when the effect of polarity couldn't be examined due to the lack of EMG data. The imbedded bar plots depict the distribution of group sum of SSMs for randomly shuffled MEPs and TEPs (Horizontal axis represents the measured SSMs and vertical axis shows the frequency of each SSM). The red line shows the group sum of the result SSMs. * indicates that $p_{uncorr} = 0.05$ (permutation test) suggesting a relationship between the two patterns. The imbedded scalp maps illustrate the distribution of the p values for SSM measurements presented; lower p values (darker colors) indicate more similarity. Among all of the evaluated conditions only PEPs-suppressed TEPs after reversing the polarity showed relationships with MEPs (electrodes highlighted in red; D).

In subthreshold stimulation, although reversing the polarity at 0–60 ms improved the SSM between the two signals and shifted the minimum p values (maximum SSMs) towards the site of stimulation, the observed relationship was not statistically significant ($p_{\text{uncorr}} = 0.38$ and $p_{\text{uncorr}} = 0.11$ before and after polarity reversal, respectively) (Fig. 10). PEP attenuation using SSP-SIR did not cause any increase in the level of similarity between the shape of the two signals ($p_{\text{uncor}} = 0.18$ and $p_{\text{uncor}} = 0.64$ before and after polarity reversal, respectively).

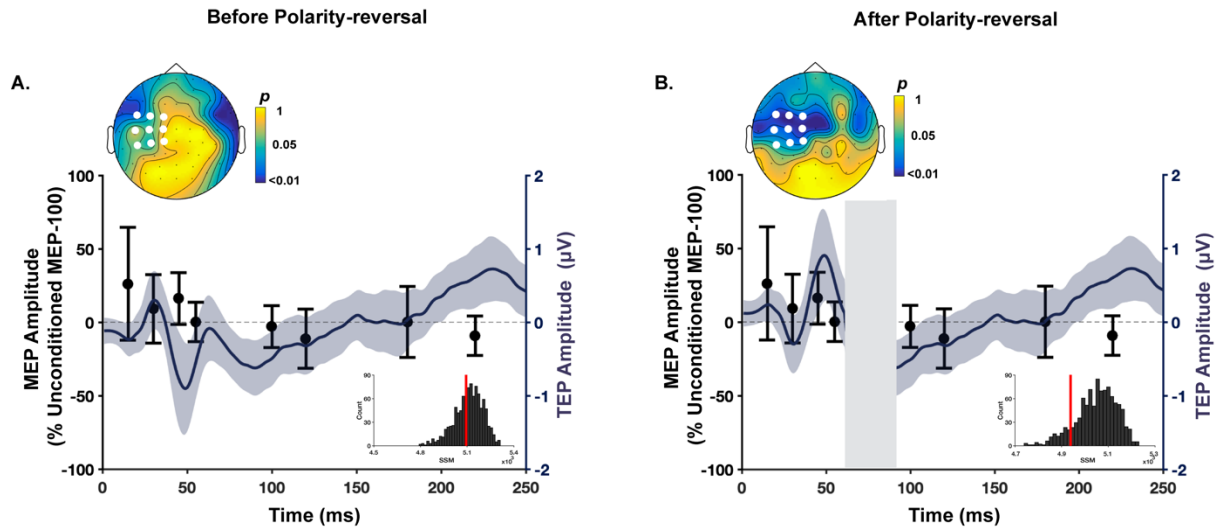


Figure 10: The relationships between local cortical responses to subthreshold TMS measured by EMG and EEG, before (A) and after (B) reversing the polarity of TEPs from 0 to 60 ms. MEPs were recorded from right FDI following ppTMS over M1 with subthreshold conditioning stimulus and suprathreshold test stimulus, and TEPs were responses to spTMS over left M1. The solid circles represent the mean amplitude of conditioned MEPs expressed as a percentage of the mean MEP amplitude from unconditioned conditioning stimulus and the error bars indicate 95% of confidence intervals. The line graphs show the average of TEPs recorded at the highlighted channels (C3, FC1, CP1, FC5, CP5, C1, FC3, CP3, C5) and the shaded areas represent the 95% of confidence intervals. The grey vertical bars show the window of time between 60 ms and 100 ms, when the effect of polarity couldn't be examined due to the lack of EMG data. The imbedded bar plots depict the distribution of group sum of SSMs for the randomly shuffled MEPs and TEPs (Horizontal axis represents the measured SSMs and vertical axis shows the frequency of each SSM). The red line shows the group sum of the result SSMs. The imbedded scalp maps illustrate the distribution of the p values for SSM measurements; lower p values (darker colors) indicate more similarity.

Discussion

In this study we examined the relationship between intracortical fluctuations following TMS over motor cortex recorded by EMG and EEG at both the local site of stimulation and within the contralateral hemisphere. We compared the amplitudes and patterns of ppTMS-MEPs and spTMS-TEPs across time using different stimulation parameters (intensity and waveform). We found that the amplitude of excitation/inhibition indexed by MEPs does not correlate with the amplitude of TEPs at any of the time points measured, except for at 15 ms when the stimulation intensity is subthreshold. Furthermore, the shape of the two signals does not follow a similar pattern when analyzing the raw signals. However, the results showed that local EEG and EMG responses to suprathreshold TMS show similar patterns when the early ($\sim < 60$ ms) TEP signal is inverted. This relationship was reproducible using both biphasic and monophasic TMS waveforms, in which different ISIs were used, and was specific to electrodes over the site of stimulation. Furthermore, the similarity observed between TEPs and MEPs was not found between MEPs and other types of event-related potentials (e.g. PEPs resulting from shoulder stimulation) and could not be obtained by changing the polarity at other time-windows. We also found that the same relationship is observable over contralateral motor cortex, but only following suppression of PEPs from the EEG signals using SSP-SIR. Our findings indicate that the neural populations responsible for fluctuations in net excitation and inhibition measured using paired-pulse MEPs and single pulse TEPs at least partially overlap, both at the site of stimulation and in remote cortical regions. This finding bridges the gap between TMS-EEG and TMS-EMG measures of cortical function and provides additional support that early TEP peaks reflect net excitation, whereas later peaks reflect net inhibition.

EMG and EEG measures of local cortical responses to TMS

A large body of evidence from both human ppTMS-EMG studies [6, 7, 36, 37] and intracellular recordings in animal [38, 39] has demonstrated that a suprathreshold TMS pulse to primary motor cortex results in a period of strong net excitation lasting between 10–30 ms followed by a period of net inhibition lasting approximately 50–200 ms at the site of stimulation. However, it is unclear whether the same pattern of response is present in other methods recording the cortical response to TMS, such as EEG, as these methods are sensitive to different scales of neural activity. For example, ppTMS-EMG mainly measures the net excitation and inhibition of a small neural population in the motor cortex representing the target muscle and is also sensitive to spinal excitability [3, 4]. On the other hand, EEG reflects synchronised fluctuations

in post-synaptic potentials across large populations of neurons in the cortex [1, 12]. Several studies have attempted to establish the location of the neural generators responsible for the different TEP peaks using various source estimation methods. The most common finding is that early TEP deflections (e.g. N15) mainly originate from the stimulated site [8, 10, 40-42], which is in line with the present results showing that N15 peak in TEPs coincides with the peak of facilitation in MEPs occurring at ISIs of 15-20 ms. Furthermore, trial-by-trial variability in the N15-P30 amplitude are related to variability in MEP amplitude, suggesting that the two measures are sensitive to overlapping cortical mechanisms [16]. As such, these findings suggest that the early negativity observed in TEPs reflects the net excitability of the stimulated cortical region. However, the cortical origin of later TEPs are less conclusive.

Following the period of net excitation, ppTMS-MEPs showed a transition to a long inhibition period (i.e. LICI) beginning at 50 ms. This transition from net excitation to net inhibition was accompanied by a shift to a large positive peak in TEPs (P60) in our data, suggesting that this positive TEP may reflect the beginning of the net inhibitory period. The strongest inhibition of MEPs occurs at ISIs of 100-120 ms, which coincided with the large N100 peak in TEPs observed in electrodes over motor cortex. Surprisingly, this finding suggests that the inhibitory period responsible for LICI in MEPs may be reflected by both positive and negative signals within the EEG. The reasons why the polarity of the EEG representing inhibition would switch over time are unclear. The location of excitatory/inhibitory inputs along the somatodendritic length of layer 5 pyramidal neurons are thought to largely determine EEG polarity [12]. Although speculative, one possible explanation is that the pyramidal neurons responsible for the EEG signal may receive inhibitory inputs to both the apical and basal dendrites across differing time scales following TMS. Certain subtypes of inhibitory cells, such as neurogliaform cells, provide spatially non-specific input to the entire surface of target cells via both synaptic and extra-synaptic GABA_A and GABA_B receptors [56, 57]. Indeed, a recent review suggested neurogliaform cells may be responsible for the long inhibition observed following TMS resulting in LICI [1], and therefore could also contribute to the EEG signal. Future work using invasive recordings in animal models is required to disentangle the precise mechanisms through which TMS interacts with cortical circuits and drives the EEG signals recorded at the scalp.

The close match between the negative TEP signals around the N100 and paired-pulse MEPs is in agreement with the several previous studies that suggest LICI of MEPs and the N100 TEP peak are both mediated by GABA_B-receptors [13, 15, 36, 43-45]. Later TEP peaks, such as the

P180 (which is actually negative in electrodes over M1 in our study) have also been suggested to represent inhibitory processes due to their similar time course with GABA_B receptors [17], relationship with motor measures of inhibition such as the cortical silent period [46], and also their positive correlations with the conditions associated with decreased inhibition, like suppression of P180 in epilepsy [17, 47]. It is worth noting that inhibition within the spinal cord, likely resulting from peripheral input following muscle movement also contributes to the inhibition of MEPs [3, 4]. However, spinal inhibition mainly occurs up to 50 ms and not beyond 100 ms post-stimulus, which would not affect most time points included in the present analysis. Furthermore, if anything, the contribution of spinal inhibition to ppTMS-MEPs would have led to an underestimation of the relationship between the MEPs and TEPs. As such, our findings show that TEPs recorded over M1 match the shape of the net early excitation and the long late inhibition observed with paired-pulse MEPs, but only when the polarity of the early EEG signal is inverted, suggesting partial overlap of the mechanisms underlying the two responses.

An important, yet unexpected, finding of the present study was that TEPs and MEPs were correlated in their shape but not amplitude. A possible explanation for this observation is that inter-individual variability in amplitudes could be driven by separate factors for each measure. While the variability in MEP amplitude between individuals has been mainly attributed to biological properties of the corticospinal tract [48, 49], variability of EEG amplitude has been linked to the morphological features of cortex and head, such as cortical thickness [50], cortical volume [51] and the distance from the active source to the scalp [52]. Therefore, biological and morphological differences across individuals could have introduced heterogeneities into TEPs and MEPs and, consequently, decoupled their amplitude.

In the subthreshold condition, we only observed a negative correlation between N15 amplitude and MEP facilitation at an ISI of 15 ms and did not find statistical similarities in shape between the two responses (although their similarity increased and shifted towards motor areas after polarity reversal similar to suprathreshold conditions; Fig. 10). There are two possible explanations for these results. First, the effect of subthreshold stimulation was small for both MEPs and TEPs, as also observed in previous studies [36, 53]. It is likely that the low signal to noise ratio of both measures decreased the power of the tests to detect the relationships between the two responses. Second, according to the findings of ppTMS-EMG studies, the largest effects of subthreshold TMS on cortical activity occur during the early post-stimulus period (ISIs < ~20 ms corresponding to short interval intracortical inhibition (SICI) and intracortical

facilitation (ICF)[1], a large part of which cannot be reliably assessed by TMS-EEG due to the presence of strong TMS artefacts [54]. Accordingly, at the earliest time point evaluated in the current study (15 ms), MEPs showed a notable facilitation (corresponding to ICF) and were negatively correlated with N15 peak amplitude in TEPs (Table 1). This finding is in line with the inverse relationship observed between the two measures in suprathreshold conditions at this time point, supporting that the N15 represents a period of excitability following both sub- and suprathreshold stimulation.

There is a growing body of evidence suggesting that some of the TEP response is driven by PEPs (mainly evoked by TMS click sounds and coil vibrations) rather than direct cortical responses to TMS, despite measures to attenuate sensory input such noise masking and foam padding. This issue appears particularly relevant for later TEP peaks (e.g. N100 and P180), which correlate strongly with sensory control conditions, especially over fronto-central electrodes [19, 20]. Importantly, the relationship between ppTMS-MEPs and spTMS-TEPs following suprathreshold stimulation observed in our study was specific to electrodes over the motor cortex (derived from both an *a priori* ROI and a data-driven ROI) and was not observed from a ROI including fronto-central electrodes. Furthermore, PEPs from a shoulder stimulation condition, which includes both auditory and somatosensory input and correlates strongly with fronto-central TEPs, did not correlate with ppTMS-MEPs. Finally, attenuating the contribution of PEPs to TEPs using SSP-SIR did not alter the relationship between TEPs and MEPs at the site of stimulation. Taken together, these findings suggest that TMS at suprathreshold intensities evokes a strong cortical response in motor cortex which is detected by electrodes over the stimulation site and is independent from TMS-evoked sensory signals.

EMG and EEG measures of the interhemispheric response to TMS

Following a TMS pulse, activity is not restricted to the stimulated cortical region but also propagates to the interconnected areas. Previous ppTMS-EMG studies demonstrated two main periods of interhemispheric inhibition (IHI) between homologous motor cortices, peaking around 10 and 30-50 ms [7, 55, 56]. The present findings show both periods of IHI in ppTMS-EMG measures, however, the first phase (10 ms) could not be compared with spTMS-EEG due to the large TMS artefacts. In our study, IHI peaked at an ISI of 30 ms, which corresponded with a large positive peak around 30 ms in TEPs over the right contralateral M1. Similar to the

findings at the site of stimulation, the patterns observed in short latency interhemispheric responses (<~60ms) followed opposite directions between MEPs and TEPs indicating the same effect of EEG polarity. However, this relationship was only evident after suppressing sensory-evoked signals using SSP-SIR. Recent findings have shown that TEP components recorded contralateral to the side of stimulation are highly correlated with TMS-induced sensory potentials, whereas TEPs at the site of stimulation mainly reflect direct cortical responses to TMS [19]. The present results confirm these findings by showing that suppressing PEPs significantly improved the relationship between the TEPs and MEPs from contralateral M1 without affecting the relationship between TEPs and MEPs at the site of stimulation. In sum, our findings suggest that the shape of spTMS-TEPs recorded at the contralateral M1 matches the shape of interhemispheric inhibition observed with ppTMS-MEPs, but only when the PEPs are suppressed, and the polarity of the early signal is inverted. This is in agreement with the results of source estimations suggesting that following suprathreshold stimulations over M1, TEPs between 20-40 ms mainly originate from the contralateral M1 [41, 42].

Conclusion

We found that fluctuations in cortical excitability following suprathreshold TMS are correlated in shape (not amplitude) when measured with EMG and EEG both at the site of stimulation and in a contralateral site. This relationship is observable only after reversing the polarity of short latency TEPs (<~60ms). For interhemispheric measures, an additional step of suppressing PEPs in TEPs is required to discern the relationship between the two responses. Together, the present findings establish a fundamental link between the periods of net excitation/inhibition measured over the stimulated and contralateral motor cortex with ppTMS-EMG and different TEP peaks. The results also highlight the importance of controlling for sensory confounds in TMS-EEG recordings, which can mask genuine TEP responses.

References

- [1] Di Lazzaro V, Rothwell J, Capogna M. Noninvasive stimulation of the human brain: activation of multiple cortical circuits. *The Neuroscientist* 2018;24(3):246-60.
- [2] Ilmoniemi RJ, Virtanen J, Ruohonen J, Karhu J, Aronen HJ, Näätänen R, et al. Neuronal responses to magnetic stimulation reveal cortical reactivity and connectivity. *Neuroreport* 1997;8(16):3537-40.
- [3] Fuhr P, Agostino R, Hallett M. Spinal motor neuron excitability during the silent period after cortical stimulation. *Electroencephalography and Clinical Neurophysiology/Evoked Potentials Section* 1991;81(4):257-62.
- [4] Ziemann U, Netz J, Szelényi A, Hömberg V. Spinal and supraspinal mechanisms contribute to the silent period in the contracting soleus muscle after transcranial magnetic stimulation of human motor cortex. *Neuroscience letters* 1993;156(1-2):167-71.
- [5] Foster AC, Kemp JA. Glutamate-and GABA-based CNS therapeutics. *Current opinion in pharmacology* 2006;6(1):7-17.
- [6] Nakamura H, Kitagawa H, Kawaguchi Y, Tsuji H. Intracortical facilitation and inhibition after transcranial magnetic stimulation in conscious humans. *The Journal of physiology* 1997;498(3):817-23.
- [7] Ni Z, Gunraj C, Nelson AJ, Yeh I-J, Castillo G, Hoque T, et al. Two phases of interhemispheric inhibition between motor related cortical areas and the primary motor cortex in human. *Cerebral Cortex* 2008;19(7):1654-65.
- [8] Bonato C, Miniussi C, Rossini P. Transcranial magnetic stimulation and cortical evoked potentials: a TMS/EEG co-registration study. *Clinical neurophysiology* 2006;117(8):1699-707.
- [9] Lioumis P, Kičić D, Savolainen P, Mäkelä JP, Kähkönen S. Reproducibility of TMS—Evoked EEG responses. *Human brain mapping* 2009;30(4):1387-96.
- [10] Komssi S, Kähkönen S, Ilmoniemi RJ. The effect of stimulus intensity on brain responses evoked by transcranial magnetic stimulation. *Human brain mapping* 2004;21(3):154-64.
- [11] Ilmoniemi RJ, Kičić D. Methodology for combined TMS and EEG. *Brain topography* 2010;22(4):233.
- [12] Jackson AF, Bolger DJ. The neurophysiological bases of EEG and EEG measurement: A review for the rest of us. *Psychophysiology* 2014;51(11):1061-71.
- [13] Ziemann U, Reis J, Schwenkreis P, Rosanova M, Strafella A, Badawy R, et al. TMS and drugs revisited 2014. *Clinical Neurophysiology* 2015;126(10):1847-68.

[14] Rogasch NC, Daskalakis ZJ, Fitzgerald PB. Mechanisms underlying long-interval cortical inhibition in the human motor cortex: a TMS-EEG study. *Journal of Neurophysiology* 2012;109(1):89-98.

[15] Premoli I, Rivolta D, Espenahn S, Castellanos N, Belardinelli P, Ziemann U, et al. Characterization of GABAB-receptor mediated neurotransmission in the human cortex by paired-pulse TMS-EEG. *Neuroimage* 2014;103:152-62.

[16] Mäki H, Ilmoniemi RJ. The relationship between peripheral and early cortical activation induced by transcranial magnetic stimulation. *Neuroscience letters* 2010;478(1):24-8.

[17] Ferreri F, Pasqualetti P, Määttä S, Ponzo D, Ferrarelli F, Tononi G, et al. Human brain connectivity during single and paired pulse transcranial magnetic stimulation. *Neuroimage* 2011;54(1):90-102.

[18] Tremblay S, Rogasch NC, Premoli I, Blumberger DM, Casarotto S, Chen R, et al. Clinical utility and prospective of TMS-EEG. *Clinical Neurophysiology* 2019.

[19] Biabani M, Fornito A, Mutanen TP, Morrow J, Rogasch NC. Characterizing and minimizing the contribution of sensory inputs to TMS-evoked potentials. *bioRxiv* 2018:489864.

[20] Conde V, Tomasevic L, Akopian I, Stanek K, Saturnino GB, Thielscher A, et al. The non-transcranial TMS-evoked potential is an inherent source of ambiguity in TMS-EEG studies. *Neuroimage* 2019;185:300-12.

[21] Rossi S, Hallett M, Rossini PM, Pascual-Leone A, Group SoTC. Safety, ethical considerations, and application guidelines for the use of transcranial magnetic stimulation in clinical practice and research. *Clinical neurophysiology* 2009;120(12):2008-39.

[22] Rossini PM, Burke D, Chen R, Cohen L, Daskalakis Z, Di Iorio R, et al. Non-invasive electrical and magnetic stimulation of the brain, spinal cord, roots and peripheral nerves: basic principles and procedures for routine clinical and research application. An updated report from an IFCN Committee. *Clinical Neurophysiology* 2015;126(6):1071-107.

[23] Rothwell J, Hallett M, Berardelli A, Eisen A, Rossini P, Paulus W. Magnetic stimulation: motor evoked potentials. *Electroencephalogr Clin Neurophysiol Suppl* 1999;52:97-103.

[24] Saatlou FH, Rogasch NC, McNair NA, Biabani M, Pillen SD, Marshall TR, et al. MAGIC: An open-source MATLAB toolbox for external control of transcranial magnetic stimulation devices. *Brain Stimulation: Basic, Translational, and Clinical Research in Neuromodulation* 2018;11(5):1189-91.

[25] Ter Braack EM, de Vos CC, van Putten MJ. Masking the auditory evoked potential in TMS-EEG: a comparison of various methods. *Brain topography* 2015;28(3):520-8.

[26] Biabani M, Fornito A, Mutanen T, Morrow J, Rogasch N. Sensory contamination in TMS-EEG recordings: Can we isolate TMS-evoked neural activity? *Brain Stimulation: Basic, Translational, and Clinical Research in Neuromodulation* 2019;12(2):473.

[27] Rogasch NC, Thomson RH, Farzan F, Fitzgibbon BM, Bailey NW, Hernandez-Pavon JC, et al. Removing artefacts from TMS-EEG recordings using independent component analysis: importance for assessing prefrontal and motor cortex network properties. *Neuroimage* 2014;101:425-39.

[28] Rogasch NC, Sullivan C, Thomson RH, Rose NS, Bailey NW, Fitzgerald PB, et al. Analysing concurrent transcranial magnetic stimulation and electroencephalographic data: a review and introduction to the open-source TESA software. *Neuroimage* 2017;147:934-51.

[29] Delorme A, Makeig S. EEGLAB: an open source toolbox for analysis of single-trial EEG dynamics including independent component analysis. *Journal of neuroscience methods* 2004;134(1):9-21.

[30] Homan RW, Herman J, Purdy P. Cerebral location of international 10–20 system electrode placement. *Electroencephalography and clinical neurophysiology* 1987;66(4):376-82.

[31] Okamoto M, Dan H, Sakamoto K, Takeo K, Shimizu K, Kohno S, et al. Three-dimensional probabilistic anatomical crano-cerebral correlation via the international 10–20 system oriented for transcranial functional brain mapping. *Neuroimage* 2004;21(1):99-111.

[32] Saxena A, Prasad M, Gupta A, Bharill N, Patel OP, Tiwari A, et al. A review of clustering techniques and developments. *Neurocomputing* 2017;267:664-81.

[33] Rousseeuw PJ. Silhouettes: a graphical aid to the interpretation and validation of cluster analysis. *Journal of computational and applied mathematics* 1987;20:53-65.

[34] Benjamini Y, Hochberg Y. Controlling the false discovery rate: a practical and powerful approach to multiple testing. *Journal of the Royal statistical society: series B (Methodological)* 1995;57(1):289-300.

[35] Michel CM, Murray MM, Lantz G, Gonzalez S, Spinelli L, de Peralta RG. EEG source imaging. *Clinical neurophysiology* 2004;115(10):2195-222.

[36] Valls-Solé J, Pascual-Leone A, Wassermann EM, Hallett M. Human motor evoked responses to paired transcranial magnetic stimuli. *Electroencephalography and Clinical Neurophysiology/Evoked Potentials Section* 1992;85(6):355-64.

[37] Kujirai T, Caramia M, Rothwell JC, Day B, Thompson P, Ferbert A, et al. Corticocortical inhibition in human motor cortex. *The Journal of physiology* 1993;471(1):501-19.

[38] Müller-Dahlhaus JFM, Liu Y, Ziemann U. Inhibitory circuits and the nature of their interactions in the human motor cortex—a pharmacological TMS study. *The Journal of physiology* 2008;586(2):495-514.

[39] Li B, Virtanen JP, Oeltermann A, Schwarz C, Giese MA, Ziemann U, et al. Lifting the veil on the dynamics of neuronal activities evoked by transcranial magnetic stimulation. *Elife* 2017;6:e30552.

[40] Mutanen TP, Kukkonen M, Nieminen JO, Stenroos M, Sarvas J, Ilmoniemi RJ. Recovering TMS-evoked EEG responses masked by muscle artifacts. *Neuroimage* 2016;139:157-66.

[41] Litvak V, Komssi S, Scherg M, Hoechstetter K, Classen J, Zaaroor M, et al. Artifact correction and source analysis of early electroencephalographic responses evoked by transcranial magnetic stimulation over primary motor cortex. *Neuroimage* 2007;37(1):56-70.

[42] Komssi S, Aronen HJ, Huttunen J, Kesäniemi M, Soinne L, Nikouline VV, et al. Ipsi- and contralateral EEG reactions to transcranial magnetic stimulation. *Clinical Neurophysiology* 2002;113(2):175-84.

[43] Premoli I, Király J, Müller-Dahlhaus F, Zipser CM, Rossini P, Zrenner C, et al. Short-interval and long-interval intracortical inhibition of TMS-evoked EEG potentials. *Brain stimulation* 2018.

[44] Premoli I, Castellanos N, Rivolta D, Belardinelli P, Bajo R, Zipser C, et al. TMS-EEG signatures of GABAergic neurotransmission in the human cortex. *Journal of Neuroscience* 2014;34(16):5603-12.

[45] McDonnell MN, Orekhov Y, Ziemann U. The role of GABA B receptors in intracortical inhibition in the human motor cortex. *Experimental brain research* 2006;173(1):86-93.

[46] Farzan F, Barr MS, Hoppenbrouwers SS, Fitzgerald PB, Chen R, Pascual-Leone A, et al. The EEG correlates of the TMS-induced EMG silent period in humans. *Neuroimage* 2013;83:120-34.

[47] Julkunen P, Säisänen L, Könönen M, Vanninen R, Kälviäinen R, Mervaala E. TMS-EEG reveals impaired intracortical interactions and coherence in Unverricht-Lundborg type progressive myoclonus epilepsy (EPM1). *Epilepsy research* 2013;106(1-2):103-12.

[48] Z'graggen W, Humm A, Durisch N, Magistris M, Rösler K. Repetitive spinal motor neuron discharges following single transcranial magnetic stimuli: a quantitative study. *Clinical neurophysiology* 2005;116(7):1628-37.

[49] Magistris MR, Rösler K, Truffert A, Myers J. Transcranial stimulation excites virtually all motor neurons supplying the target muscle. A demonstration and a method improving the study of motor evoked potentials. *Brain: a journal of neurology* 1998;121(3):437-50.

[50] Provencher D, Hennebelle M, Cunnane SC, Bérubé-Lauzière Y, Whittingstall K. Cortical thinning in healthy aging correlates with larger motor-Evoked EEG desynchronization. *Frontiers in Aging Neuroscience* 2016;8:63.

[51] Schwarzkopf DS, Robertson DJ, Song C, Barnes GR, Rees G. The frequency of visually induced gamma-band oscillations depends on the size of early human visual cortex. *Journal of Neuroscience* 2012;32(4):1507-12.

[52] Butler R, Bernier P-M, Mierzwinski GW, Descoteaux M, Gilbert G, Whittingstall K. Cortical distance, not cancellation, dominates inter-subject EEG gamma rhythm amplitude. *NeuroImage* 2019.

[53] Gordon PC, Desideri D, Belardinelli P, Zrenner C, Ziemann U. Comparison of cortical EEG responses to realistic sham versus real TMS of human motor cortex. *Brain stimulation* 2018;11(6):1322-30.

[54] Rogasch NC, Thomson RH, Daskalakis ZJ, Fitzgerald PB. Short-latency artifacts associated with concurrent TMS-EEG. *Brain stimulation* 2013;6(6):868-76.

[55] Ferbert A, Priori A, Rothwell J, Day B, Colebatch J, Marsden C. Interhemispheric inhibition of the human motor cortex. *The Journal of physiology* 1992;453(1):525-46.

[56] Daskalakis ZJ, Christensen BK, Fitzgerald PB, Roshan L, Chen R. The mechanisms of interhemispheric inhibition in the human motor cortex. *The Journal of physiology* 2002;543(1):317-26.